



**Cite this article:** Kemp LR, Dunstan MS, Fisher K, Warwicker J, Leys D. 2013 The transcriptional regulator CprK detects chlorination by combining direct and indirect readout mechanisms. *Phil Trans R Soc B* 368: 20120323.  
<http://dx.doi.org/10.1098/rstb.2012.0323>

One contribution of 12 to a Theme Issue 'Organohalide respiration: using halogenated hydrocarbons as the terminal electron acceptor'.

**Subject Areas:**

biochemistry, biophysics, microbiology, molecular biology, structural biology

**Keywords:**

CprK, organohalide respiration, transcriptional regulation, phenol  $pK_a$ , green fluorescent protein, halogen detection

**Author for correspondence:**

David Leys

e-mail: [david.leys@manchester.ac.uk](mailto:david.leys@manchester.ac.uk)

Electronic supplementary material is available at <http://dx.doi.org/10.1098/rstb.2012.0323> or via <http://rstb.royalsocietypublishing.org>.

# The transcriptional regulator CprK detects chlorination by combining direct and indirect readout mechanisms

Laura R. Kemp, Mark S. Dunstan, Karl Fisher, Jim Warwicker and David Leys

Faculty of Life Sciences, Manchester Institute of Biotechnology, University of Manchester, 131 Princess Street, Manchester M1 7DN, UK

The transcriptional regulator CprK controls the expression of the reductive dehalogenase CprA in organohalide-respiring bacteria. *Desulfitobacterium hafniense* CprA catalyses the reductive dechlorination of the terminal electron acceptor *o*-chlorophenol acetic acid, generating the phenol acetic acid product. It has been shown that CprK has ability to distinguish between the chlorinated CprA substrate and the de-halogenated end product, with an estimated an estimated  $10^4$ -fold difference in affinity. Using a green fluorescent protein GFP<sub>UV</sub>-based transcriptional reporter system, we establish that CprK can sense *o*-chlorophenol acetic acid at the nanomolar level, whereas phenol acetic acid leads to transcriptional activation only when approaching micromolar levels. A structure–activity relationship study, using a range of *o*-chlorophenol acetic-acid-related compounds and key CprK mutants, combined with  $pK_a$  calculations on the effector binding site, suggests that the sensitive detection of chlorination is achieved through a combination of direct and indirect readout mechanisms. Both the physical presence of the bulky chloride substituent as well as the accompanying electronic effects lowering the inherent phenol  $pK_a$  are required for high affinity. Indeed, transcriptional activation by CprK appears strictly dependent on establishing a phenolate–K133 salt bridge interaction, rather than on the presence of a halogen atom *per se*. As K133 is strictly conserved within the CprK family, our data suggest that physiological function and future applications in biosensing are probably restricted to phenolic compounds.

## 1. Introduction

While halide chemistry is a mainstay of modern chemical synthesis and products, the presence of halide atoms within biological molecules is a relatively rare occurrence [1,2]. Indeed, the presence of halide atoms in xenobiotic molecules often renders them recalcitrant to biological mineralization and can cause or augment toxic effects. The high toxicity, persistence and bioaccumulation of chlorinated molecules such as polychlorinated biphenyls (PCBs) or dioxins is of particular concern, and pollution of the environment and/or food chain by these compounds is often exacerbated by detection problems [3,4]. Organohalide-respiring bacteria have been shown to use a range of chlorinated molecules as terminal electron acceptors, and these organisms as well as the molecular components underpinning this process have the potential for future applications in bioremediation/biosensing of PCB/dioxin-type compounds [5]. *Desulfitobacterium* are strictly anaerobic, low-G + C bacteria, belonging to the Firmicutes, Clostridia and Peptococcaceae [6] and have been studied for over a decade because of their ability to dehalogenate organic compounds via organohalide respiration. The bacterium *Desulfitobacterium hafniense* DCB-2 is able to dechlorinate many chlorinated compounds including: pentachlorophenol (PCP), tetrachloroethene and 3-chloro-4-hydroxyphenylacetic acid (OCPA) [7,8]. The key enzymes that catalyse the final reduction step are known as reductive

dehalogenases (Rdhs). Rdh enzymes are predicted to be membrane anchored by a small protein and are corrinoid/iron-sulfur-containing proteins. CprA Rdh isolated from *Desulfitobacterium* species are able to dechlorinate a range of halogen-substituted phenolic compounds [9–11]. In *D. dehalogenans* and *D. hafniense*, the CprA genes are under tight transcriptional control by the regulator CprK [9]. CprK belongs to the CRP/FNR family of regulators and, following binding to the effector *o*-chlorophenol acetic acid, binds a specific DNA promoter sequence within the *cpr* gene cluster called a dehalobox (TTAAT–N<sub>4</sub>–ATTA) [12–17].

The CRP/FNR family of transcription regulators is ubiquitous in bacteria and is able to respond to a wide spectrum of signals from within the cell and its environment [18,19]. All members of this superfamily contain an N-terminal sensor module able to bind the effector—OCPA in the case of CprK—or undergo effector-mediated modification. Allosteric effects of ligand binding or modification of the N-terminal sensor domain is transmitted to the C-terminal DNA-binding domain through the central pair of  $\alpha$ -helices that connect both domains and form a large part of the dimer interface. The exact allosteric networks that underpin the regulator function are distinct for each of those family members that have been studied in molecular detail (i.e. CooA, CprK, CRP) reflecting the versatility in the type of signal/ligand sensed (respectively CO gas, cAMP, halogenated phenolic compounds; for reviews see [18,19]). Furthermore, the dimeric nature of the CRP/FNR family members appears to be exploited differently depending on the type of signal sensed. In the case of CRP, mild negative cooperativity between both binding sites is hypothesized to allow the molecule to report on a wide range of cAMP concentrations, as both the half and fully occupied dimers (each with distinct DNA-binding affinities) are populated to significant levels [20]. By contrast, it has been proposed that CprK exhibits either extreme positive or no cooperativity, both effectively leading to an equilibrium between unbound and fully bound CprK [16]. In the latter case, this presumably reflects the need for CprK to function as a single threshold on-off switch.

CprK displays remarkable ability to distinguish between the halogenated OCPA and the corresponding non-halogenated 4-hydroxyphenylacetic acid (HPA), estimated from indirect *in vitro* measurements at 10<sup>4</sup> difference in affinity [13–16]. This not only ensures the reductive dehalogenase is only produced when substrate is present, but also avoids an accumulation of the product from the dehalogenation reaction leading to persistent signalling. Detailed structural information on CprK in a range of states has revealed that OCPA binds to the effector domain central  $\alpha$ -helix pair interface, with concomitant rigid body reorientation of the effector domain with only minor changes in residues lining the ligand-binding site. The chloride atom is located in a hydrophobic pocket at the central  $\alpha$ -helix pair surface (formed by Y130, L131, K133, V134). No directional halogen bonding contacts can be observed [21]. The relatively weak nature of these hydrophobic contacts and the fact these residues only undergo minor changes upon ligand binding appears inconsistent with the marked difference in affinity and response displayed by CprK towards OCPA and HPA. We proposed that in addition to detecting the presence of the halogen atom directly, through hydrophobic contacts, CprK senses the pK<sub>a</sub> of the phenolic moiety [14,16]. The phenol group is

within hydrogen bonding distance of Y76, the backbone NH of G85 and the conserved K133, with a potential salt bridge forming between the deprotonated phenolate group and K133 (figure 1). The nature of this network would depend on the pK<sub>a</sub> of the phenolic moiety, which is influenced by the presence of the halogen atom. In this study, we describe the *in vivo* transcriptional activation levels of wild-type (WT) CprK and a number of selected mutants for a range of OCPA-like effector molecules, combined with calculations of the K133/phenol protonation states within the crystal structures. Our data reveal a pivotal role for K133 and establish a link between phenol pK<sub>a</sub> and effector affinity. We furthermore reveal that the presence of a phenol group, rather than the halogen substituent itself, is the key prerequisite for transcriptional activation by CprK.

## 2. Results and discussion

### (a) Development of a GFP<sub>UV</sub>-based effector reporter assay

Previous studies have shown that OCPA-dependent transcriptional activation by CprK can be monitored in *Escherichia coli* [17,22]. To avoid any effects coupled to the redox state of the cell, we used a CprK C200S mutant as the basis for all our studies (referred to hereafter as CprK), as it was previously shown that oxidative disulfide bond formation involving C200 inactivates the regulator [23]. A region comprising 123 nucleotides of the upstream dehalobox promoter region of CprA1, containing CprK binding element dehalobox 7 (DB7), was cloned into pGFP<sub>UV</sub> in order to create a novel *in vivo* reporter system that makes use of an optimized variant of the green fluorescent protein (GFP<sub>UV</sub>) from *Aequorea victoria*. Fluorescence levels of the pGFP<sub>UV</sub>-DB7 containing *E. coli* cells were comparable to non-transformed cell-lines indicating minimal basal transcription of GFP (figure 2). No significant increase in fluorescence levels could be detected in the presence of OCPA or similar compounds. Fluorescence levels for cells containing both pGFP<sub>UV</sub>-DB7 and pET28a-CprK were comparable to the pGFP<sub>UV</sub>-DB7 single transformants, indicating negligible levels of transcriptional activation occur in the absence of the halogenated effector. By contrast, addition of 0.6  $\mu$ M OCPA to the media leads to a nearly 10-fold increase in fluorescence levels, indicating CprK-mediated, OCPA-dependent transcriptional activation of the GFP<sub>UV</sub> gene occurs within the *E. coli* host. Although a comparison with published  $\beta$ -galactosidase-based assays reveals the amplification level achieved using GFP<sub>UV</sub> to be significantly smaller (over a 20-fold increase has been reported [17,22]), the pGFP<sub>UV</sub>-DB7 system allows for a more accurate and direct *in vivo* observation of protein expression levels. We measured fluorescence levels as a function of OCPA concentration in the medium and found a sigmoidal dependence in the data that could be fitted to a Hill equation, with a Hill coefficient of  $n = 2.0 \pm 0.2$  and an apparent K<sub>d</sub> of  $0.019 \pm 0.002 \mu$ M (figure 3 and table 1). Our apparent K<sub>d</sub> is the binding constant calculated as the concentration at which effector induces half F<sub>max</sub> (maximum fluorescence). Our apparent K<sub>d</sub> data are significantly smaller than that previously reported *in vitro* for OCPA (K<sub>d</sub> = 0.8–3.5  $\mu$ M) [13–16]. In contrast to the direct measurement of formation of the CprK : OCPA complex for the *in vitro* experiment, the *in vivo* data probably report on the formation of the (CprK : OCPA : dehalobox : RNA polymerase) quaternary complex. Indeed, it was found that the CprK

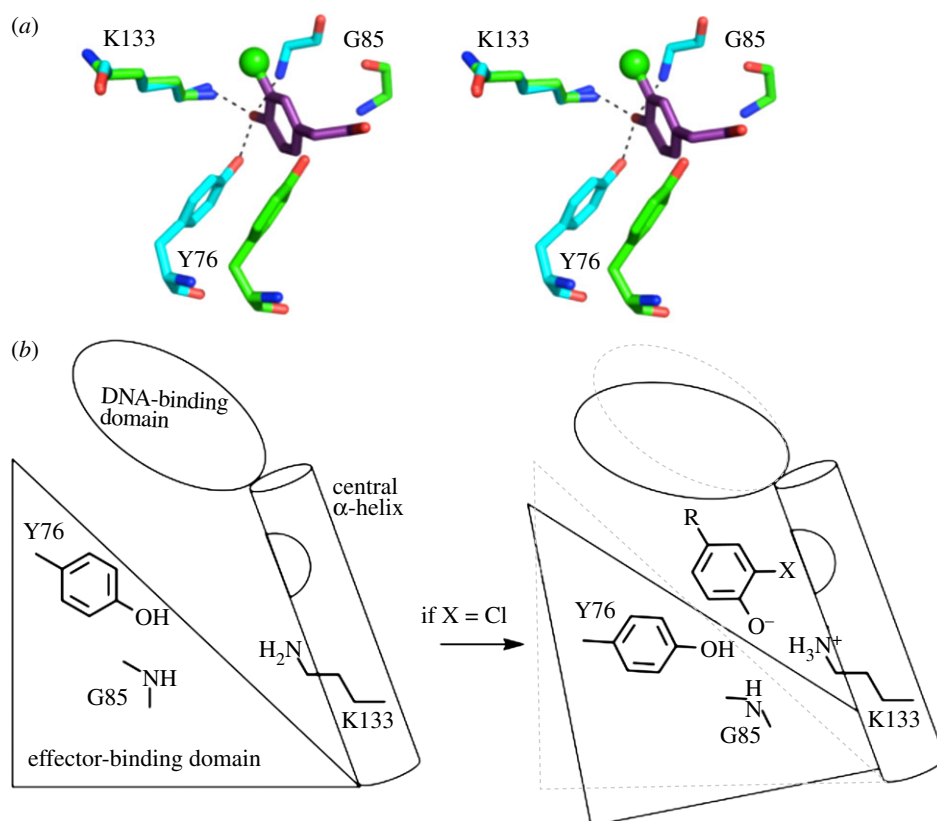


**Figure 1.** (a) Stereo view of an overlay of the CprK effector binding site in the OCPA-bound (with cyan carbon atoms) and unbound (green carbon atoms) conformations. The OCPA chloride atom is shown as a green sphere, and the remainder of the effector molecule as atom coloured sticks (purple carbon atoms). (b) Schematic of the proposed CprK mechanism. CprK is presented as a single monomer for clarity; for a more detailed schematic that includes the proposed cooperativity between CprK monomers, see Joyce *et al.* [14].

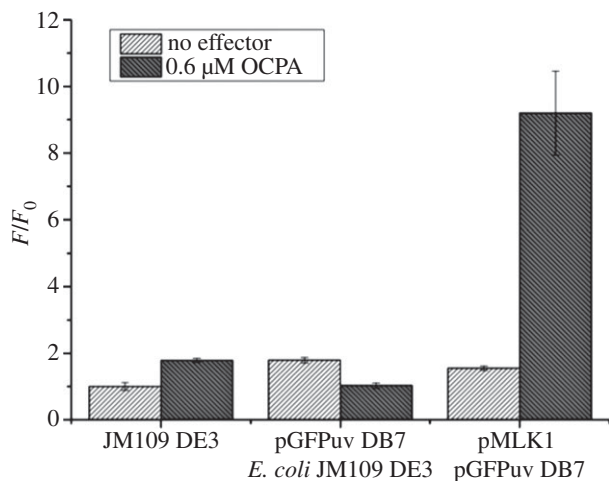


**Figure 2.** GFP<sub>UV</sub>-DB7 reporter assay. Ratio of fluorescence levels at  $t = 3$  h/ $t = 0$  in the presence and absence of  $0.6 \mu\text{M}$  OCPA obtained for *E. coli* JM109 DE3 cells, containing either no plasmid, pGFP<sub>UV</sub>-DB7 only or co-transformed with pGFP<sub>UV</sub>-DB7 and pMLK1. Fluorescence values are normalized to cell density levels. Error bars indicate the standard deviation of three separate readings.

affinity for OCPA was increased approximately 10-fold when in the presence of a DNA promoter fragment [13]. It appears that under the conditions used for the pGFP<sub>UV</sub>-DB7-based system, the apparent  $K_d$  for OCPA is approximately 100-fold smaller than the established *in vivo*  $K_d$  values. Furthermore, the *in vivo* data could only be accurately modelled using a Hill equation, revealing positive cooperative behaviour that has not previously been observed for *in vitro* experiments. It is important to keep in mind that transport processes could affect the intracellular OCPA

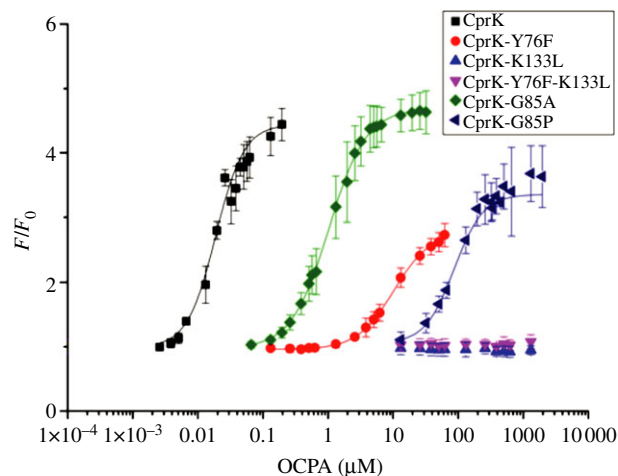


**Figure 3.** Fluorescence levels are depend on OCPA concentration. The ratio of fluorescence of pGFP<sub>UV</sub>-DB7 *E. coli* JM109 DE3 cells expressing either CprK or selected mutant versions, incubated at various OCPA concentrations for 3 h to the fluorescence values are normalized to cell density levels. Error bars indicate the standard deviation of three separate readings.

concentrations across the membrane, although it would seem logical to assume this would affect OCPA and OCPA-like components in a similar manner. To confirm the apparent  $K_d$  value observed reflects inherent CprK affinity for the effector molecule, we measured the increase in fluorescence levels for a range of aromatic compounds. The relationship between the nature of the aromatic compounds tested and the apparent  $K_d$  obtained strongly suggests that these experiments directly probe inherent CprK affinity.

**Table 1.** Apparent *in vivo*  $K_d$  for OCPA determined for CprK and selected mutant forms.

CprK	$K_d$ (apparent; $\mu\text{M}$ )	$n$	adj. $R^2$
CprK	$0.019 \pm 0.002$	$2.0 \pm 0.2$	0.988
K133L	no response	n.a.	n.a.
Y76F	$10.2 \pm 0.9$	$1.6 \pm 0.1$	0.996
G85A	$1.03 \pm 0.06$	$1.5 \pm 0.1$	0.998
G85P	$86.7 \pm 5.8$	$1.9 \pm 0.3$	0.995

### (b) Substitution of the OCPA *ortho*-functional group affects *in vivo* transcriptional activation by CprK

Figure 4 and table 2 show apparent  $K_d$  values and associated Hill constants for a range of 4-hydroxyphenylacetic acid molecules with different *o*-substituents (Br, Cl, F, H). The relative difference in atomic radius of the four distinct *o*-substituents can only partly explain the observed trend in associated  $K_d$  values. There is an approximately 10 000-fold difference in  $K_d$  between OCPA and HPA, according to previously determined, albeit indirect, estimations of the discriminatory power of CprK for the substrate and product [14,16]. The atomic radius of the *o*-substituent clearly plays a role in this mechanism, but is not the only determinant. In this respect, the 40-fold difference between apparent  $K_d$  values for HPA and *o*-3-fluoro-4-hydroxyphenyl acetic acid (*o*-FPA) is noteworthy, as H and F have a very similar atomic radius but have distinct electronegativity. This supports the  $pK_a$  interrogation hypothesis for the mechanism of CprK, as the  $pK_a$  between HPA and *o*-FPA is affected by the F-substituent. To explore the relationship between atomic radius of the PA *o*-functional group and CprK affinity in the absence of significant  $pK_a$  effects, we tested a range of *p*-nitrophenolic compounds. In this series, the electron-withdrawing effects of the *p*-nitro substituent largely determine the phenol  $pK_a$ .

### (c) Both atomic radius and electronegativity of the phenylacetic acid *ortho*-functional group determine CprK affinity

Table 2 and figure 4 show apparent  $K_d$  values and associated Hill constants for a range of *p*-nitrophenolic compounds ( $\text{CH}_3$ , Br, Cl, F and H as *o*-substituent). Unlike the PA series, the  $pK_a$  of the *p*-nitrophenol series is largely determined by the nitro-group. A comparison between OCPA and the corresponding *o*-chloro-*p*-nitrophenol reveals approximately a 20-fold difference in affinity, probably owing to the loss of hydrogen bonding interactions with the acetic acid moiety. Within the *p*-nitrophenol series, there is a clear trend between atomic radius of the *o*-substituent and the corresponding apparent  $K_d$ . An approximately sevenfold difference between *o*-methyl-*p*-nitrophenol and *p*-nitrophenol reveals that atomic radius plays a significant part in the CprK mechanism, as both C and H have very similar electronegativity values. These data support the hypothesis that CprK determines the nature of the *o*-substituent through both direct effects (atomic radius through van der Waals interactions) and indirect effects (hydrogen bonding network and salt bridge to the phenolate moiety). To investigate whether CprK has the ability to function with

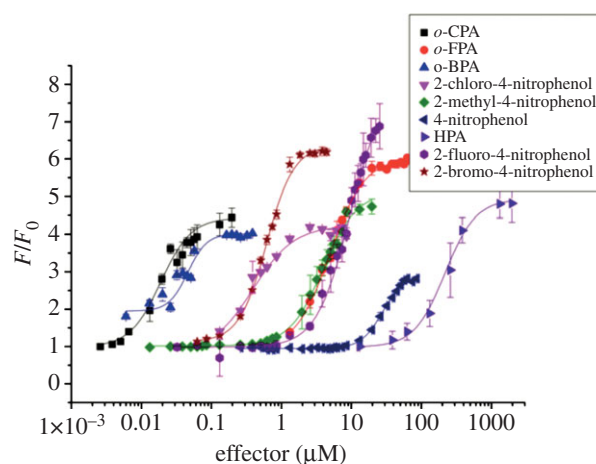


**Figure 4.** Fluorescence levels depend on the nature of the phenolic effector. The ratio of fluorescence of pGFP<sub>UV</sub>-DB7 *E. coli* JM109 DE3 cells expressing WT CprK1, incubated at various concentrations of a phenolic effector for 3 h to the fluorescence obtained at  $t = 0$ . Fluorescence values are normalized to cell density levels. Error bars indicate the standard deviation of three separate readings.

non-phenolic effector molecules, we investigated the effects of *o*-chloro-*p*-nitroaniline and of 3-chloro-phenylacetic acid on fluorescence levels.

### (d) Only phenolic compounds elicit transcriptional activation by CprK

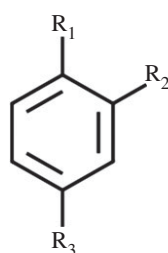
No increase in fluorescence levels could be observed for a range of aniline compounds such as *o*-chloro-*p*-nitroaniline, or 3-chloro-phenylacetic acid, a molecule highly similar to OCPA but lacking the phenolic group (table 2). It is interesting to note that the *D. hafniense* strain PCP-1 is able to dechlorinate pentachloroaniline and 2,3,5,6-tetrachloroaniline, but only after induction by 3,5-dichlorophenol and 2,4,6-trichlorophenol [24]. In the case of 3-chloro-phenylacetic acid, a lack of apparent binding can easily be explained by the loss of the hydrogen bonding network and the K133 salt bridge to the phenolate moiety. Furthermore, the lack of any effect on fluorescence levels for *o*-chloro-*p*-nitroaniline suggests this polar network of interactions cannot be established with an  $-\text{NH}_2$  group. In this respect, the relative difference between  $-\text{NH}_2$  and  $-\text{OH}$  (phenol) or  $-\text{O}^-$  (phenolate), respectively, would support the hypothesis that CprK binds only to the phenolate form. The phenolate group is within hydrogen bonding distance of Y76, backbone NH of G85 and K133 (figure 1), putatively receiving a hydrogen bond from each amino acid and establishing a salt bridge with the conserved K133. The fact that the latter amino acid is strictly conserved in CprK paralogues suggests a common role in their recognition of (halogenated) phenolic effectors. By contrast, Y76 is not conserved, and a previous study has revealed a Y76F mutation leads to an approximately 10-fold decrease in the  $K_d$  for OCPA, consistent with the interruption of a single hydrogen bond [14]. To further probe the relative contributions made by each amino acid to the phenolate-binding polar network, we studied the properties of Y76F, G85A, G85P and K133L CprK mutants.

### (e) The conserved K133 is crucial to CprK functionality

Table 1 and figure 3 show the dependence of fluorescence levels on OCPA concentrations for Y76F, G85A, G85P and

**Table 2.** Apparent *in vivo*  $K_d$  for a range of aromatic compounds for CprK. For general structure of effectors, see figure 5.

effector	$R_1$ ( $pK_a$ value)	$R_2$	$R_3$	apparent $K_d$ ( $\mu\text{M}$ )	$n$	adj. $R^2$
4-hydroxyphenylacetic acid (HPA)	–OH (10.2)	–H	–CH <sub>2</sub> –COOH	$210 \pm 17$	$2.1 \pm 0.2$	0.995
3-fluoro-4-hydroxyphenylacetic acid	–OH (8.8)	–F	–CH <sub>2</sub> –COOH	$4.96 \pm 0.26$	$1.8 \pm 0.2$	0.998
3-chloro-4-hydroxyphenylacetic acid (OCPA)	–OH (8.5)	–Cl	–CH <sub>2</sub> –COOH	$0.019 \pm 0.002$	$2.0 \pm 0.2$	0.988
3-bromo-4-hydroxyphenylacetic acid	–OH (8.5)	–Br	–CH <sub>2</sub> –COOH	$0.046 \pm 0.003$	$3.2 \pm 0.5$	0.967
4-nitrophenol	–OH (7.2)	–H	–NO <sub>2</sub>	$27.7 \pm 1.5$	$2.8 \pm 0.2$	0.993
2-fluoro-4-nitrophenol	–OH (5.7)	–F	–NO <sub>2</sub>	$10.0 \pm 1.2$	$4.7 \pm 0.6$	0.998
2-chloro-4-nitrophenol	–OH (5.5)	–Cl	–NO <sub>2</sub>	$0.402 \pm 0.050$	$1.7 \pm 0.2$	0.999
2-bromo-4-nitrophenol	–OH (5.5)	–Br	–NO <sub>2</sub>	$0.613 \pm 0.016$	$2.1 \pm 0.1$	0.999
2-methyl-4-nitrophenol	–OH (7.4)	–CH <sub>3</sub>	–NO <sub>2</sub>	$3.92 \pm 0.33$	$1.8 \pm 0.1$	0.993
4-nitroaniline	–NH <sub>2</sub>	–H	–NO <sub>2</sub>	no binding	n.a.	n.a.
2-chloro-4-nitroaniline	–NH <sub>2</sub>	–Cl	–NO <sub>2</sub>	no binding	n.a.	n.a.
2-methyl-4-nitroaniline	–NH <sub>2</sub>	–CH <sub>3</sub>	–NO <sub>2</sub>	no binding	n.a.	n.a.
3-chloro-phenylacetic acid	–H	–Cl	–CH <sub>2</sub> –COOH	no binding	n.a.	n.a.

**Figure 5.** General structure of the effectors used in this study.

K133L CprK mutants. Western blot analysis of the soluble cell fractions transformed with CprK WT or mutant expression plasmids reveals similar levels of soluble CprK protein in the cell (data not shown). Compared with the apparent  $K_d$  of WT CprK ( $0.019 \pm 0.002 \mu\text{M}$ ) for OCPA, the Y76F mutant has an approximately 500-fold decreased affinity for OCPA. The G85P mutation leads to an even more dramatic 4500-fold decrease, but this is probably not only a consequence of removal of the backbone NH hydrogen bond, but also because of the increased size and restricted conformational freedom of the proline side chain. In this respect, the more conservative mutation G85A, which does not remove the possibility of a hydrogen bond between the phenolate and position 85 and reveals the extra presence of a methyl group, already significantly affects OCPA affinity, leading to an approximately 50-fold activity decrease. While mutations at position 76 or 85 retain some activity, mutation at position 133 leads to a complete loss of transcriptional activation response. This clearly establishes K133 as the key contributor to the polar network established with the phenol moiety.

#### (f) $pK_a$ calculations for the CprK effector binding site

We used computational modelling to provide further insight into CprK effector binding by modelling  $pK_a$  and protonation values for K133 and the OCPA or HPA phenolic group, respectively. We used available crystal structures to model a

K133L mutant structure, as well as a putative complex of the WT protein with HPA. Table 3 shows the average protonation state of K133 and the OCPA phenolic group, averaged over both effector sites within the CprK dimer, at pH 7.5 for the different CprK complexes (i.e. 1 = protonated, 0 = deprotonated). The most striking feature of calculated protonations for effector sites is that K133 and phenol protonations sum to 1. These titratable sites are adjacent within a relatively low dielectric environment, shielded from bulk water, leading to strong interaction and tight coupling. However, the strong interaction between protonated K133 and the deprotonated phenolate is largely balanced by the desolvation penalties associated with these ionizations. As a result, the location of the shared proton is predicted to shift from K133 to phenol according to the phenol  $pK_a$ . Thus, for OCPA complexes, the balance lies towards the ion pair, whereas for a putative HPA–CprK complex, the balance is predicted to be towards the neutral pair. In the absence of the ligand, but within the ligand-bound protein conformation context, K133 is predicted to be unprotonated. For a modelled K133L mutation, the phenol group of the bound effector is predicted to be protonated, emphasizing the tight coupling of K133 and phenol groups. These calculations are consistent with the  $pK_a$  readout hypothesis for effector binding to CprK. The effector binding site is poised, in terms of K133/phenol charge distribution, and we estimate a contribution of around 5 kJ per mole more favourable for a single OCPA than a single HPA, at pH 7.5.

### 3. Conclusions

Since their discovery a few decades ago, organohalide-respiring bacteria have been studied to determine the biochemical basis for their unusual metabolism, recently culminating in the genome sequence of a range of model species [25,26]. The unusual nature of the substrate, a halogenated molecule, presents these organisms with new challenges for which they have

**Table 3.** Average protonation state of K133 and the OCPA/HPA phenolic group, averaged over both effector sites within the CprK dimer, at pH 7.5 (i.e. 1 denotes protonated; 0 denotes deprotonated).

CprK structure	K133 protonation	phenol protonation	K133 + phenol protonation
apo-structure (PDB code 3e5q)	0.7	n.a.	n.a.
binary OCPA complex (3e5x)	0.9	0.1	1.0
ternary OCPA and DNA complex (3e6c)	0.8	0.2	1.0
3e5x-derived model binary HPA complex	0.4	0.6	1.0
3e6c-derived model for ternary HPA and DNA complex	0	1.0	1.0
3e5x-based binary OCPA K133L model	n.a.	1.0	1.0
3e5x-derived apo-structure (in binary complex conformation)	0	n.a.	n.a.

**Table 4.** Strains and plasmids used in this study.

strain/ or plasmid	relevant characteristics	origin of replication	promoter	reference
<i>E. coli</i>				
DH5 $\alpha$	<i>fhuA2</i> $\Delta$ ( <i>argF-lacZ</i> )U169 <i>phoA glnV44</i> $\Phi$ 80 $\Delta$ ( <i>lacZ</i> )M15 <i>gyrA96 recA1 relA1 endA1 thi-1 hsdR17</i>			New England Biolabs
JM109 (DE3)	<i>endA1, recA1, gyrA96, thi, hsdR17</i> ( <i>r<sub>k</sub><sup>-</sup>, m<sub>k</sub><sup>+</sup></i> ), <i>relA1, supE44, <math>\lambda</math>-</i> , $\Delta$ ( <i>lac-proAB</i> ), [ <i>F'</i> , <i>traD36, proAB, lacI<sup>q</sup>Z</i> $\Delta$ M15], IDE3			Promega
pET28a(+)	Km <sup>R</sup> , pET28a(+)	f1, ColE1	T7	Novagen
pMLK1	<i>D. hafniense cprK<sub>C200S</sub></i> cloned into pET28a	f1, ColE1	T7	this study
pMLK2	<i>D. hafniense cprK<sub>C200S-K133L</sub></i> cloned into pET28a	f1, ColE1	T7	this study
pMLK3	<i>D. hafniense cprK<sub>C200S-Y76F</sub></i> cloned into pET28a	f1, ColE1	T7	this study
pMLK4	<i>D. hafniense cprK<sub>C200S-G85A</sub></i> cloned into pET28a	f1, ColE1	T7	this study
pMLK5	<i>D. hafniense cprK<sub>C200S-G85P</sub></i> cloned into pET28a	f1, ColE1	T7	This study
pGFP <sub>UV</sub>	Am <sup>R</sup> , pGFP <sub>UV</sub>	pUC	lac	[27]
pGFP <sub>UV</sub> -DB7	dehalobox promoter cloned into pGFP <sub>UV</sub>	pUC	DB7	this study

found corresponding novel biochemical solutions [5]. This, combined with the potential for a future application in bioremediation/biosensing of halogenated xenobiotics of these organisms, warrants a detailed investigation of the organohalide respiratory process. Although a range of transcriptional regulators have been implicated in the organohalide respiration process, reflecting the wide range of compounds used as electron acceptors, CprK is the only protein for which a wealth of biochemical data are available. This transcriptional regulator has the ability to distinguish between the chlorinated effector and the corresponding non-halogenated component by an approximately 10 000-fold difference in affinity. Our *in vivo* measurement of apparent  $K_d$  establishes that CprK has the potential to sense halogenated molecules at nanomolar levels, and directly confirms the striking difference between OCPA and HPA affinity. Furthermore, by studying the effects of substitution of key CprK amino acids or OCPA substituents, we have been able to confirm that this is due to a combination of both direct and indirect readout mechanisms. While the physical presence of the halogen substituent contributes to affinity via van der Waals interactions, the main detection mechanism appears indirect: sensing the effects of the electro-negative halogen substituent on the phenol  $pK_a$ . Indeed,

transcriptional activation by CprK is entirely dependent on the presence of K133 and a phenolic effector molecule, rather than the strict presence of a halogen atom *per se*.  $pK_a$  calculations of the CprK effector binding site indeed support the proposal that an ionic interaction is formed between K133 and the effector. The fact that K133 is strictly conserved within the CprK family suggests its function is limited to sensing the presence of halogenated phenolic components in the environment. We would thus predict that application of CprK family members or variants in biosensing is likely to remain limited to phenolic compounds.

## 4. Material and methods

### (a) Strains, plasmids and growth conditions

Characteristics of the strains and plasmids used in this study are listed in table 4. *Escherichia coli* DH5 $\alpha$  cells were used as a host for mutagenized plasmids. *Escherichia coli* JM109 DE3 cells were used for co-transformations and GFP assay. Origins of replication of co-transformed plasmids were within the same incompatibility group (table 4), but in possession of different selective markers. It has been shown that it is possible to maintain

**Table 5.** Oligonucleotides used in this study.

oligonucleotide name	oligonucleotide sequence	template	plasmid created
CprK K133L F	CTTTAAAACTACCTTACCAAAGTGGCTTATTATGCGCGAC	pMLK1	pMLK2
CprK K133L R	GTCGCGCATAATAAGCCACTTTGGTAAGGTAGTTTTAAAG	pMLK1	pMLK2
CprK Y76F F	GCTTCTCTTTTATGCCGGCGGC	pMLK1	pMLK3
CprK Y76F R	GCCGCCGGCATAAAAGAGAAGC	pMLK1	pMLK3
CprK G85A F	GGCAATCCCTGATCGAAAATTATATCTACG	pMLK1	pMLK4
CprK G85A R	CGTAGGATATAATTTTGCATCAGGAATTGCC	pMLK1	pMLK4
DB7 GFP F	GACTGGAAGCAGATCTGCTCTGGG	<i>D. hafniense</i> DCB-2 genomic DNA	p-GFP <sub>UV</sub> -DB7
DB7 GFP R	GTGAAATTTATGATATCAAAAAGTAG	<i>D. hafniense</i> DCB-2 genomic DNA	p-GFP <sub>UV</sub> -DB7

high-copy vectors from the same incompatibility group, with differing selective markers in *E. coli* over the course of 5 days [28]. In order to maximize plasmid survival, cells were co-transformed, and assays completed within 5 days. Kanamycin (30  $\mu\text{g ml}^{-1}$ ) was used as a selective agent for transformations of mutagenized plasmids. Ampicillin (100  $\mu\text{g ml}^{-1}$ ) was used as a selective agent for cloning of pGFP<sub>UV</sub>-DB7. Kanamycin (30  $\mu\text{g ml}^{-1}$ ) and ampicillin (100  $\mu\text{g ml}^{-1}$ ) were used as selective agents for co-transformation of CprK-derived and GFP-containing plasmids. CprK-derived genes were under the basal control of a T7 promoter, in the absence of isopropyl  $\beta$ -D-1-thiogalactopyranoside. Cells were grown in LB broth or agar at 37°C.

### (b) Recombinant DNA techniques

All oligonucleotides used for PCR are listed in table 5. Plasmid isolation, digestion with restriction endonucleases, site-directed mutagenesis by PCR and transformation into *E. coli* were performed by standard methods [29,30].

### (c) *In vivo* GFP<sub>UV</sub>-coupled activity assay

Overnight culture (150  $\mu\text{l}$ ) was plated onto 96-well optical bottom plates (Nunc). OCPA-related compounds (table 3) were then added to various end concentrations, and the plates placed on a rotary shaker at 37°C for 3 h. GFP fluorescence levels were measured using a Synergy HT microplate reader (BioTek) using a 400 nm, 30 nm bandpass excitation filter and a 508 nm, 20 nm bandpass emission filter. Data were collected using Gen5 v. 1.05 (Biotek) software. Fluorescence was normalized against cell density and measured by absorbance at 600 nm. The fluorescence ratio was plotted against effector concentration, and apparent  $K_d$  of binding was calculated using nonlinear curve fitting to a Hill plot.

### (d) Western blot analysis of CprK soluble protein levels

To assess cellular levels of soluble CprK variants used in *in vivo* GFP-coupled activity assays, 1.5 ml of overnight culture was pelleted by centrifugation, and the supernatant was discarded. The pellet was resuspended with 300  $\mu\text{l}$  BugBuster protein extraction reagent (Merck), supplemented with 10  $\mu\text{g ml}^{-1}$  lysozyme, 10  $\mu\text{g ml}^{-1}$  DNase and 10  $\mu\text{g ml}^{-1}$  RNase. The mixture was incubated at 21°C, 300 r.p.m., for 10 min. The lysed cells were centrifuged at 10 000g 4°C, for 10 min. Soluble fractions were collected and concentrations determined using a Bradford assay (Sigma). The soluble fractions were added to SDS-loading buffer to a final amount of 30  $\mu\text{g}$  protein. The proteins were then electro-transferred onto Immobilon PVDF membrane (Millipore), and detected using Universal His Western blotting kit 2 (Clontech).

### (e) $pK_a$ calculations

Calculations of  $pK_a$  values were made with an implementation of the finite difference Poisson–Boltzmann method [31]. Relative dielectric values were assigned as 4 (protein) and 78.4 (water), with an ionic strength of 0.15 M, and amino acid model compound  $pK_a$  values as in previous work [31]. OCPA was assigned a  $pK_a$  of 8.5 and HPA 10.2. Energetics of pH-dependence were calculated according to Antosiewicz *et al.* [32]. The unbound dimer of CprK was used (3e5q) in binary complex with effector (3e5x), and ternary complex with effector and DNA (3e6c). In order to compare calculated K133  $pK_a$  with that for the true unbound structure, a calculation was also made for the notional unbound form of CprK dimer extracted from the binary complex. The K133L mutant was modelled in Swiss PDB viewer [33].

This research was supported by a BBSRC studentship to L.R.K. and an ERC starter grant no. (DEHALORES 206080) to D.L.

## References

- Gribble GW. 2003 The diversity of naturally produced organohalogenes. *Chemosphere* **52**, 289–297. (doi:10.1016/S0045-6535(03)00207-8)
- Zhang XJ, Lai TB, Kong R. 2012 Biology of fluoro-organic compounds. *Top. Curr. Chem.* **308**, 365–404. (doi:10.1007/128\_2011\_270)
- Larsen JC. 2006 Risk assessments of polychlorinated dibenzo-*p*-dioxins, polychlorinated dibenzofurans, and dioxin-like polychlorinated biphenyls in food. *Mol. Nutr. Food Res.* **50**, 885–896. (doi:10.1002/mnfr.200500247)
- Marnane I. 2012 Comprehensive environmental review following the pork PCB/dioxin contamination incident in Ireland. *J. Environ. Monitor.* **14**, 2551–2556. (doi:10.1039/C2EM30374D)
- Smidt H, de Vos WM. 2004 Anaerobic microbial dehalogenation. *Annu. Rev. Microbiol.* **58**, 43–73. (doi:10.1146/annurev.micro.58.030603.123600)
- Villemur R, Lanthier M, Beaudet R, Lépine F. 2006 The *Desulfitobacterium* genus. *FEMS Microbiol. Rev.* **30**, 706–733. (doi:10.1111/j.1574-6976.2006.00029.x)
- Madsen T, Licht D. 1992 Isolation and characterization of an anaerobic chlorophenol-transforming bacterium. *Appl. Environ. Microbiol.* **58**, 2874–2878.
- Christiansen N, Ahring BK. 1996 *Desulfitobacterium hafniense* sp. nov.: an anaerobic, reductively dechlorinating bacterium. *Int. J. Syst. Bacteriol.* **46**, 442–448. (doi:10.1099/00207713-46-2-442)
- van de Pas BA, Smidt H, Hagen WR, van der Oost J, Schraa G, Stams AJM, de Vos WM. 1999 Purification and molecular characterization of ortho-chlorophenol

- reductive dehalogenase, a key enzyme of halo-respiration in *Desulfitobacterium dehalogenans*. *J. Biol. Chem.* **274**, 20 287–20 292. (doi:10.1074/jbc.274.29.20287)
10. Bisaillon A, Beaudet R, Lépine F, Déziel E, Villemur R. 2010 Identification and characterization of a novel CprA reductive dehalogenase specific to highly chlorinated phenols from *Desulfitobacterium hafniense* strain PCP-1. *Appl. Environ. Microbiol.* **76**, 7536–7540. (doi:10.1128/AEM.01362-10)
  11. Thibodeau J, Gauthier A, Duguay M, Villemur R, Lépine F, Juteau P, Beaudet R. 2004 Purification, cloning, and sequencing of a 3,5-dichlorophenol reductive dehalogenase from *Desulfitobacterium frappieri* PCP-1. *Appl. Environ. Microbiol.* **70**, 4532–4537. (doi:10.1128/AEM.70.8.4532-4537.2004)
  12. Smidt H, van Leest M, van der Oost J, de Vos WM. 2000 Transcriptional regulation of the cpr gene cluster in ortho-chlorophenol-respiring *Desulfitobacterium dehalogenans*. *J. Bacteriol.* **182**, 5683–5691. (doi:10.1128/jb.182.20.5683-5691.2000)
  13. Pop S, Kolarik R, Ragsdale S. 2004 Regulation of anaerobic dehalorespiration by the transcriptional activator CprK. *J. Biol. Chem.* **279**, 49910–49918. (doi:10.1074/jbc.M409435200)
  14. Joyce MG *et al.* 2006 CprK crystal structures reveal mechanism for transcriptional control of halo-respiration. *J. Biol. Chem.* **281**, 28318–28325. (doi:10.1074/jbc.M602654200)
  15. Mazon H, Gábor K, Leys D, Heck A, van der Oost J, van den Heuvel R. 2007 Transcriptional activation by CprK1 is regulated by protein structural changes induced by effector binding and redox state. *J. Biol. Chem.* **282**, 11281–11290. (doi:10.1074/jbc.M611177200)
  16. Levy C, Pike K, Heyes DJ, Joyce MG, Gabor K, Smidt H, van der Oost J, Leys D. 2008 Molecular basis of halo-respiration control by CprK, a CRP-FNR type transcriptional regulator. *Mol. Microbiol.* **70**, 151–167. (doi:10.1111/j.1365-2958.2008.06399.x)
  17. Gabor K, Verissimo CS, Cyran BC, ter Horst P, Meijer NP, Smidt H, de Vos WM, van der Oost J. 2006 Characterization of CprK1, a CRP/FNR-type transcriptional regulator of halo-respiration from *Desulfitobacterium hafniense*. *J. Bacteriol.* **188**, 2604–2613. (doi:10.1128/jb.188.7.2604-2613.2006)
  18. Körner H, Sofia HJ, Zumft WG. 2003 Phylogeny of the bacterial superfamily of Crp-Fnr transcription regulators: exploiting the metabolic spectrum by controlling alternative gene programs. *FEMS Microbiol. Rev.* **27**, 559–592. (doi:10.1016/S0168-6445(03)00066-4)
  19. Green J, Scott C, Guest J. 2001 Functional versatility in the CRP-FNR superfamily of transcription factors: FNR and FLP. *Adv. Microbial Physiol.* **44**, 1–34. (doi:10.1016/S0065-2911(01)44010-0)
  20. Popovych N, Sun S, Ebright RH, Kalodimos CG. 2006 Dynamically driven protein allostery. *Nat. Struct. Mol. Biol.* **13**, 831–838. (doi:10.1038/nsmb1132)
  21. Auffinger P, Hays FA, Westhof E, Ho PS. 2004 Halogen bonds in biological molecules. *Proc. Natl Acad. Sci. USA* **101**, 16 789–16 794. (doi:10.1073/pnas.0407607101)
  22. Gabor K, Hailesellasse Sene K, Smidt H, de Vos WM, van der Oost J. 2008 Divergent roles of CprK paralogues from *Desulfitobacterium hafniense* in activating gene expression. *Microbiology* **154**, 3686–3696. (doi:10.1099/mic.0.2008/021584-0)
  23. Gupta N, Ragsdale SW. 2008 Dual roles of an essential cysteine residue in activity of a redox-regulated bacterial transcriptional activator. *J. Biol. Chem.* **283**, 28 721–28 728. (doi:10.1074/jbc.M800630200)
  24. Dennie D, Gladu I, Lepine F, Villemur R, Bisaillon JG, Beaudet R. 1998 Spectrum of the reductive dehalogenation activity of *Desulfitobacterium frappieri* PCP-1. *Appl. Environ. Microbiol.* **64**, 4603–4606.
  25. Kube M, Beck A, Zinder SH, Kuhl H, Reinhardt R, Adrian L. 2005 Genome sequence of the chlorinated compound-respiring bacterium *Dehalococcoides* species strain CBDB1. *Nat. Biotechnol.* **23**, 1269–1273. (doi:10.1038/nbt1131)
  26. Taş N, Van Eekert MHA, De Vos WM, Smidt H. 2010 The little bacteria that can: diversity, genomics and ecophysiology of ‘*Dehalococcoides*’ spp. in contaminated environments. *Microbial Biotechnol.* **3**, 389–402. (doi:10.1111/j.1751-7915.2009.00147.x)
  27. Feilmeier BJ, Iseminger G, Schroeder D, Webber H, Phillips GJ. 2000 Green fluorescent protein functions as a reporter for protein localization in *Escherichia coli*. *J. Bacteriol.* **182**, 4068–4076. (doi:10.1128/JB.182.14.4068-4076.2000)
  28. Velappan N, Sblattero D, Chasteen L, Pavlik P, Bradbury ARM. 2006 Plasmid incompatibility: more compatible than previously thought? *Protein Eng. Design Selection* **20**, 309–313. (doi:10.1093/protein/gzm005)
  29. Ausubel FM, Brent R, Kingston RE, Moore DD, Seidman JG, Smith JA, Struhl K, eds. 1989 *Current protocols in molecular biology*. New York, NY, USA: Greene Publishing and Wiley Interscience.
  30. Ho SN, Hunt HD, Horton RM, Pullen JK, Pease LR. 1989 Site-directed mutagenesis by overlap extension using the polymerase chain reaction. *Gene* **77**, 51–59. (doi:10.1016/0378-1119(89) 90358-2)
  31. Warwicker J. 2004 Improved pK<sub>a</sub> calculations through flexibility based sampling of a water-dominated interaction scheme. *Protein Sci.* **13**, 2793–2805. (doi:10.1110/ps.04785604)
  32. Antosiewicz J, McCammon JA, Gilson MK. 1994 Prediction of pH-dependent properties of proteins. *J. Mol. Biol.* **238**, 415–436. (doi:10.1006/jmbi.1994.1301)
  33. Guex N, Peitsch MC. 1997 SWISS-MODEL and the Swiss-Pdb viewer: an environment for comparative protein modeling. *Electrophoresis* **18**, 2714–2723. (doi:10.1002/elps.1150181505)